The 5th PSU-UNS International Conference on Engineering and Technology (ICET-2011), Phuket, May 2-3, 2011
Prince of Songkla University, Faculty of Engineering
Hat Yai, Songkhla, Thailand 90112
78

THEORETICAL ANALYSIS OF QUASI-STATIC COMPRESSION OF HEXAGONAL RING

M.R. Said[1*] and A. S Tahir[1]
[1]Faculty of Mechanical Engineering,
Universiti Teknikal Malaysia Melaka, Malaysia
*Authors to correspondence should be addressed via email: radzai@utem.edu.my

Abstract: *This paper presents a study on the load-compression and energy absorption characteristics of a laterally crushed across faces of hexagonal ring with constraints on expansion perpendicular to the loading axis. The theoretical analysis in compression across faces is developed using Equivalent Structure Technique. Experimental observations are compared with theoretical analyses and good agreements are seen.*

Keywords: *Hexagonal ring, energy absorption, finite element analysis*

1. INTRODUCTION

Much research and development has taken place in the area of impact energy absorbers. The energy absorption capacity of a circular ring under lateral compression was first addressed by Mutchler [1]. Two different kinematically admissible collapse mechanisms which result in same post-collapse load-deflection characteristic when employing a rigid perfectly-plastic material model were put forward by DeRuntz and Hodge [2] and Burton and Craig [3]. Careful and exhaustive experiments on the crushing of tubes and rings [4] led to the formation of a model that is based on the classical elastica theory that used a rigid linear strain hardening material behaviour [5]. However, by preventing the horizontal diameter of the ring from increasing, the formation of more plastic hinges is required. Reddy and Reid [6] examined the behaviour of laterally compressed tubes under transverse constraints and noticed that the collapse load increased by a factor approximately 2.4 and the energy absorbed increased by a factor of 3 in comparison with transversely unrestrained tubes. An excellent review of the energy absorbing systems, which use the lateral compression of metal tubes is given by Reid [7,8]. While, Leu [9] simulated aluminium tube under lateral compression using finite element modelling.

Plastic collapse of square tubes compressed laterally between two plates was studied by Sinha and Chitkara [10] who produced plastic collapse mechanisms. Gupta and Ray [11] have performed experiments on thin-walled empty and filled square tubes laterally compressed by using a rigid platen. They analysed the problem with the Sinha and Chitkara [10] mechanisms and assumed plastic hinges occurred only at mid section of vertical side, while in horizontal side to be elastic bending. These analyses used plastic hinges and could be modified by replacing plastic hinges with plastic zones [12]. Johnson and Reid [13] cited the energy absorbing devices with hexagonal shapes referring to an article of Fuse and Fukuda [14] where in hexagonal tubes under quasi-static compression across faces were studied. The mechanism of collapse has hinges at the side corners and at the centres of loaded faces. Recently, Said and Reddy [15] developed a predicted load-displacement curve using upperbound analysis and found that the collapse load is in good agreement with experiment but deviate 20% - 25% after the post collapse.

In the present study, theoretical study has been given on a single hexagonal ring with side constraints subjected to compression across faces, by using equivalent structure technique [16]. The experimental results on the load-displacement are also compared. is developed and compared with experimental results [17,18].

2. ANALYSIS OF COMPRESSION A CROSS FACES WITH SIDE CONSTRAINTS

The Equivalent Structure Technique demonstrated successfully by Gill [16] and are used by Reddy and Reid [6] for a circular ring compressed diametrically with transverse constraints, is used. Owing to symmetry, only one half of the ring is considered. Friction between the tube and top and bottom platens is neglected. The material of the tube is assumed to be rigid-perfectly plastic and any interactions between bending and normal or shear stress resultants are neglected. The material is made of mild steel. Modulus of Elasticity, E is 212 GPa. The yield stress, σ_y and poisson ratio, v is 212 GPa and 0.27, respectively.

Figure 1 shows two possible modes of deformation for one half of a hexagonal ring compressed vertically

across faces and restrained laterally. There are three distinct phases in each mode. In mode 1, the link AGE is assumed as a rigid in all three phase, while in mode 2, AGE remains rigid only in phase 1 and GEC is assumed to be a rigid link in phase 2 and 3. However, mode 1 shows close correlation with the experimental observation[18]. Thus, the analysis is based on mode 1.
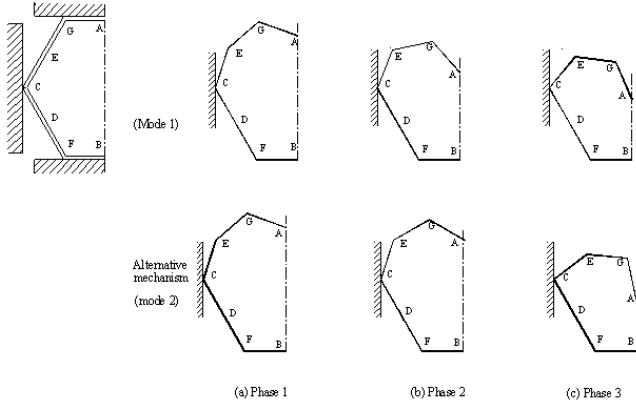

Figure 1: The possibility of deforming mode of hexagonal ring, compressed across faces: mode 1 and mode 2
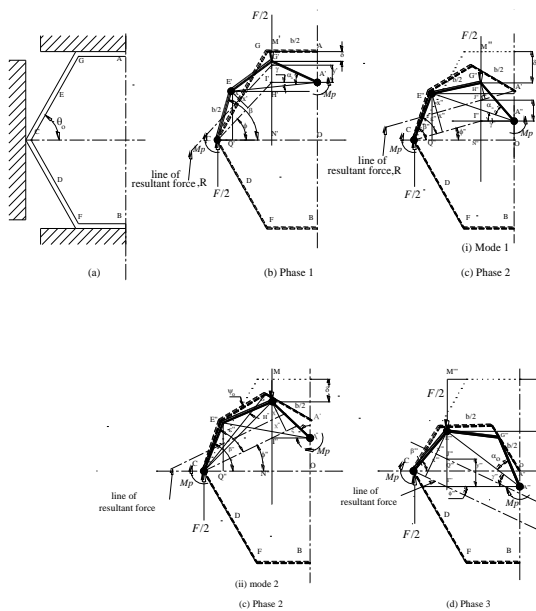

Figure 2 : Crushing across the faces of a transversely constrained hexagonal ring. (a) undeformed (b), (c), and (d) show different phases during deformation. Dotted and broken lines indicate the initial configuration and the starting positions for the respective phases.

The bottom half remains rigid in all three phases. The first phase starts with the formation of 3 hinges at A', E', and C'. The load acts at points G, A moves down and moves in vertical with E' as centre. This continues until the two hinges A' and E' at the same horizontal level as shown by the broken lines in Figure 2c. Further deformation proceeds (in phase 2, mode 1) with the stationary hinge A'' moving down, the geometry compatibility being facilitated by the reversal of the direction of rotation about C. This continues until A'' is the same level with C. The third phase is shown

in Figure 2d. The phase ends as link CE''' becomes horizontal.

2.1. Analysis of Phase 1

Figure 2b shows a general position in phase 1. The load is acting at G' and the position is defined by a deflection, δ. $A'G'E'$ remains rigid and the links rotate at about plastic hinges at A', E' and C. AE inclined at 30° to the horizontal before deformation (i.e $\alpha_o = 30°$), is now inclined at an angle γ. If I' is the point of intersection of vertical line through G' and the horizontal line through A', the line of action of the resultant force, R is parallel to CI'. The equivalent structure for $CE'G'$ should be parallel to the line of action of the resultant force and equidistant from C and E', causing fully plastic moments ($\pm M_p = \frac{\sigma_y t^2 w}{4}$) at these points. The horizontal component of this resultant force with a moment arm $I'J'$ will be responsible for the plastic bending moment at A'. The bending moment at A' is also can be checked and equal to M_p. The horizontal component of R is $H = R \cos \phi$ and this acts with a moment arm $y' = I'J' = x'/\cos\phi$ and hence the moment at A' is $H y' = R x' = M_p$.

The various angles defining the geometry at the instant shown are given in Figure 2b. CI' and hence the line of action of the resultant force is inclined at an angle ϕ to the horizontal. For a given β leads to the displacement δ of,

$$\delta = M'N - G'T' - H'I' - H'N' \qquad (1)$$

where

$$M'N' = b \sin \theta_o$$
$$G'I' = \frac{b}{2} \sin(\alpha_o - \gamma); \qquad G'A' = \frac{b}{2}$$
$$H'I' = b \cos \alpha_o \sin \gamma; \qquad E'A' = b \cos \alpha_o$$

and

$$H'N' = E'Q' = \frac{b}{2} \sin \beta$$

Therefore,

$$\delta = b \sin \theta_o - \frac{b}{2} \sin(\alpha_o - \gamma) - b \cos \alpha_o \sin \gamma - \frac{b}{2} \sin \beta \qquad (2)$$

It can be shown from geometry that γ and β are related by $CQ' + Q'O = CO$ as

$$\cos\beta = \frac{\left(\frac{b}{2}+b\cos\theta_o\right)-2\left(\frac{b}{2}\right)\cos\alpha_o\cos\gamma}{\frac{b}{2}}$$

$$=1+2\cos\theta_o-2\cos\alpha_o\cos\gamma \qquad (3)$$

The resultant force to cause fully plastic bending moments at C and E' is

$$R = \frac{M_p}{x'}$$

because $\frac{F}{2}=R\sin\phi$ and $2x''=\frac{b}{2}\sin\varepsilon$, then $\qquad (4)$

$$F = \frac{8M_p\sin\phi}{b\sin\varepsilon} \qquad (5)$$

where $\varepsilon=\beta-\phi$ and $\tan\phi=\dfrac{I'N'}{C'N'}=\dfrac{b\cos\alpha_o\sin\gamma+\frac{b}{2}\sin\beta}{b-\frac{b}{2}\cos(\alpha_o-\gamma)}$ $\quad(6)$

Phase 1 ends when hinges E' and A' at the same horizontal level, i.e. $\gamma=0°$. At this instant, noting that $\phi=40.35°$, it can be seen that $\varepsilon=34.11°$ and this $\beta=74.46°$ from equation (6). The deflection, δ at the end of phase 1 obtained from equation (2) is $0.1343b$ as $\alpha_o=30°$ and $\theta_o=60°$.

The load-deflection trace represented by equations 2 and 5 is shown in Figure 3. The experimental load-deflection curves are also compared [18].

2.2 Phase 2- Mode 1

Figure 2c(i) shows the mode of deformation in phase 2. The hinge A' continues to move down along the vertical line, to A'', $A''G''E''$ remains rigid while CE'' rotates about hinge C. In this phase, E'' will be the instantaneous centre of rotation of $A''G''E''$. The end of this mode of deformation occurs when, A'' is at the same level as C. The line of resultant force is parallel to CI'' and is equidistant from C and E''.

$$\delta = M''N''-G''H''-H''N'' \qquad (7)$$

$$\delta = b\sin\theta_o -\frac{b}{2}\sin(\alpha_o-\gamma'')\frac{b}{2}\sin\beta'' \qquad (8)$$

It can be shown from geometry that γ'' and β'' are related by $CQ''+Q''O=CO$, as

$$\cos\beta'' = \frac{\left(\frac{b}{2}+b\cos\theta_o\right)-b\cos\alpha_o\cos\gamma''}{\frac{b}{2}}$$

$$=1+2\cos\theta_o-2\cos\alpha_o\cos\gamma'' \qquad (9)$$

The resultant forces and resisting moment are related by, $R=\dfrac{M_p}{x''}$ and the applied and resultant forces by

$$\frac{F}{2}=R\sin\phi'' \qquad (10)$$

hence,

$$F=\frac{8M_p\sin\phi''}{b\sin\varepsilon''} \qquad (11)$$

where as before

$$\sin\varepsilon'' = \frac{2x''}{\frac{b}{2}};\varepsilon''=\beta''-\phi'' \text{ and} \qquad (12)$$

$$\tan\phi'' = \frac{I''N''}{C''N''}=\frac{H''N''-H''I''}{C''N''}$$

$$=\frac{\frac{b}{2}\sin\beta''-\left\{\frac{b}{2}\sin(\alpha_o+\gamma'')\frac{b}{2}\sin(\alpha_o-\gamma'')\right\}}{\frac{b}{2}\cos\beta''+\frac{b}{2}\cos(\alpha_o-\gamma'')} \qquad (13)$$

End of phase 2 is when point A'' and C are at the same level. At this instant $\gamma''=30^O$, $\phi''=0°$, $\varepsilon''=\beta''=60^O$ and $\delta=0.43b$. The bending moment at A'' can also be checked and found to be equal to M_p during this phase. The horizontal component of R is $R\cos\phi''$ acts with a moment arm $y''=I''J''=x''/\cos\phi''$ and hence the moment at A'' is M_p. It also can be shown that bending moment at G'' is always less than M_p as distance n is always less than x''.

The load-deflection curve represented by equations 8 and 11 is plotted in Figure 3.

2.3 Phase 2- Mode 2

In an alternative mode, as shown in Figure 2c(ii), point G'' travels downward and a plastic hinge is formed at G''. The link $E''G''C$ is assumed to be rigid (hence $\psi_O=22.22^O$ as at the end of phase 1) until hinge A'' is the same level with hinge C.

The deflection referring to Figure 2c(ii) is

$$\delta = M\,''N\,''- G\,''N\,'' \tag{14}$$

where,

$$M\,''N\,'' = b\sin\theta_o$$

$$G\,''N\,'' = CG\,''\sin(\beta\,''-\psi_o); CG\,'' = 2\left(\frac{b}{2}\cos\psi_o\right)$$

Therefore,

$$\delta = b\sin\theta_o - \sin\cos\psi_o\sin(\beta\,''-\psi_o) \tag{15}$$

It can be shown from the triangle $CG''I''$ that

$$G\,''I\,'' = \frac{b\cos\psi_o}{\sin(90+\phi\,'')}\sin(\beta\,''-\psi_o-\phi\,'') \tag{16}$$

The resulting force to cause fully plastic bending at C

and G'' is

$$R = \frac{M_p}{x\,''} \tag{17}$$

We have as before

$$\frac{F}{2} = R\sin\phi\,'' \text{ and } 2x\,'' = G''I'\cos\phi\,'' = \frac{b\cos\psi_o\,\sin(\beta\,''-\psi_o-\phi\,'')}{\sin(90+\phi\,'')}\cos\phi\,''$$

$$\ldots\ldots(18)$$

Combining equations (17) and (18) give

$$F = \frac{4M_p\sin\phi\,''}{b\cos\psi_O\sin(\beta\,''-\psi_O-\phi\,'')} \tag{19}$$

Mode 2 in phase 2 terminates at $\phi\,'' = 0, \varepsilon\,'' = \beta\,'' = 52^o$ and $\delta = 0.41b$. The bending moment at is found to be Mp.

The load-displacement of equations 15 and 19 is plotted in Figure 3.

2.4 Phase 3

This phase starts with hinge A'' at point O and at the same level with hinge C. At this instant, the point of load application $F/2$ has shifted to point E''' which as shown in Figure 3. The link $A'''G'''E'''$ is assumed to remain rigid and hinge A''' continues to move down along the vertical line facilitated by rotation about C and E'''. This phase continues until CE''' becomes horizontal. For a given $\beta\,'''$ leads to the displacement,δ of,

$$\delta = M\,'''N\,'''- E\,'''Q\,'''$$
$$= b\sin\theta_o - \frac{b}{2}\sin\beta\,''' \tag{20}$$

Now, $F = 2R\sin\phi\,''', \quad R = \dfrac{M_p}{x\,'''} \tag{21}$

where, $2x\,''' = E'''I'''\cos\phi\,'''$,

as $E'''I''' = A''E'''\sin\gamma\,'''$; $A''E''' = b\cos\alpha_o$

$\gamma\,'''$ can be obtained from the condition,

$b = CO = CQ''' + A''I'''$ as

$$\cos\gamma\,''' = \frac{1}{\cos\alpha_o}\left(1 - \frac{\cos\beta\,'''}{2}\right) \tag{22}$$

$\phi\,'''$ can be obtained from the compatibility of $Q'''I'''$

$$\tan\phi\,''' = \frac{Q'''I'''}{CQ'''} = \frac{E'''I''' - E'''Q'''}{CQ'''} \tag{23}$$

where,

$$E'''I''' = A''E''\sin\gamma\,''', EQ'' = \frac{b}{2}\sin\beta\,''' \quad and \quad CQ'' = \frac{b}{2}\cos\beta\,'''$$

then,

$$\tan\phi\,''' = \frac{2\cos\alpha_0\sin\gamma\,''' - \sin\beta\,'''}{\cos\beta\,'''} \tag{24}$$

Hence,

$$F = \frac{8M_p\sin\phi\,'''}{b\sin(\phi\,''' + \beta\,''')} \tag{25}$$

End of phase 3 is when CE''' becomes horizontal, i.e. $\beta\,''' = 0$. At this instant, $\phi\,''' = 54.7^o, \gamma\,''' = 54.7^o$ and $\delta = 0.866b$. The horizontal component of resultant force is $R\cos\phi\,'''$ acts with a moment arm $y\,''' = I'''J''' = x\,'''/\cos\phi\,'''$ and hence the moment at A''' is Mp.

The load-deflection curves of the third phase in equations 20 and 25 are plotted in Figure 3.

3 DISCUSSION

The analysis in section 2 is an idealisation of reality. The aspects not included in the analysis are friction, interaction of bending and normal or shear stress resultants, aspect of material properties, dimensional variations and at the corners initially during deformation at plastic zones. This gives a slight deviation on load-

displacement curve compared with the experimental result. It also assumes that the deforming mode is symmetrical about the vertical axis but in experiment this is not observed. Figure 3 shows the comparison between analyses and experimental results on load-displacement curve compressed across faces. The predicted collapse loads are infinite as moment arms are zero in the idealised cases (phase 1 in Figure 3). The zero load observed in the analysis is due to the fact that the line of action of the resultant force becomes horizontal and hence the vertical component is zero (end of second phase in Figure 3). The predicted load-displacement curves in the first phase for the case of compressed across faces seem to have the same form as the experimental curve (Figure 3) in which the load drops very fast within 5 mm displacement.
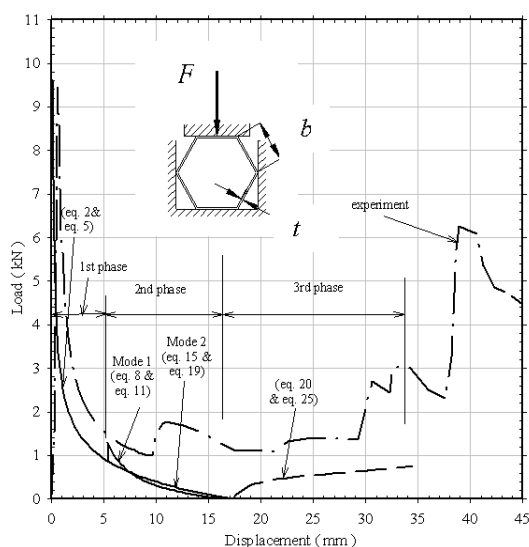

Figure 3:Comparison between analytical and experiment load-displacement curve for lateral compression hexagonal rings across faces with side constraints ($b = 40$mm, $t = 1.87$mm, $w = 10$mm)

However, the theoretical valley load underestimates the experiments up to 50% in compression across faces. This could be due to the effect of changes in the geometry resulting from strain hardening and neglect of the interaction of bending, normal and shear stress resultants in the analysis. The neglect of frictional effects in the analysis between the side constraints and ring faces also contributes to the differences between theory and experiment in the appropriate post collapse regimes. In addition, the analysis assumes symmetrical deformations, but the lack of symmetry in experiment is obvious particularly in the later stages.

4 CONCLUSION

The theoretical analysis produces good results in phase 1 when compressed across faces. If friction and strain hardening effects are introduced in the analysis, the result may be close to experiment.

5 REFERENCES

[1] Mutchler, L. D., Energy absorption in aluminium tubing. *J. Applied Mech*, 27, 1960,pp. 740-743.

[2] DeRuntz & Hodge., Crushing of a tube between rigid plates. *J. Applied. Mech*, 30,1963, pp. 391-395

[3] Burton, R. H., & Craig, J. M., An investigation into the energy absorbing properties of metal tubes loaded in the transverse direction. *B.Sc. Report*, University of Bristol, 1963.

[4] Reddy, T.Y., & Reid, S.R., Phenomena associated with the crushing of metal tubes between rigid plates. *Int. J. Solids and Structures,* 16, 1980, pp.545,

[5] Reid, S.R., & Reddy, T.Y., Effect of strain hardening on the lateral compression of tubes between rigid plates. *Int. J. Solid and Structures,* 14, 1978,pp. 213-225

[6] Reddy, T.Y., & Reid, S.R., Lateral compression of tubes and tube-systems with side constraints. *Int. J Mech. Sci*, 21, 1979,pp. 187-199

[7] Reid, S.R., Laterally compressed metal tubes as impact energy absorber. In: Jones N. and Wierzbicki T. Editors. *Structural Crashworthiness*, Butterworth, 1983,pp. 1-43

[8] Reid, S.R., Metal tubes as impact absorbers. In: Reid S. R. Editor. *Metal Forming and Impact Mechanics,* Pergamon Press, 1985,pp 249-269

[9] Leu, D.K., Finite-element simulation of lateral compression of aluminium tube between rigid plates. *lnt J Mech Sci,* 41, 1990,pp. 621-638

[10]Sinha, D.K., & Chitkara, N.R., Plastic collapse of square rings. *Int. J. Solid Structure*, 18(18), 1982,pp. 819-826

[11]Gupta, N. K., & Ray, P., Collapse of thin-walled empty and filled square tubes under lateral loading between rigid plates. *Int J Crashworthiness*, 3(3), 1998,pp. 265-285

[12]Reddy, T.Y., Impact energy absorption using laterally compressed metal tubes. *PhD Thesis*, Depart of Eng, University of Cambridge, England, 1978.

[13]Johnson, W., & Reid, S. R., Metallic Energy Dissipating Systems. *Applied Mechanics Reviews*, 31(3), 1978,pp. 277-288

[14]Fuse, H., & Fukuda, H., Plastic deformation characteristics of polygonal cross section cylinders. Meiji University Dept. of Eng, Rpt. No. 26-27, 1973,I-62, 31

[15]Said, M. R., & Reddy, T.Y., Quasi-static response of laterally simple compressed hexagonal rings. *Int J Crashworthiness*, 7(3), 2002,pp. 345-363

[16]Gill, S.S., Large deflection rigid-plastic analysis of a built-in semi-circular arch. *Int. J. of Mech. Eng,* 4, 1976,pp. 339

[17]Said, M. R., Reddy, T.Y., & Ahmad, R., The accuracy of finite element method on hexagonal ring under lateral loading. *ICAST2003*, 2003, pp. 361-364

[18]Said, M. R., Ahmad, R., Alias, A., & Md Akil, H., The deformation of hexagonal ring with side constraints under quasi-static loading.Proceedings of 2nd International Conference on Structure Processing and Properties of Material *SPPM2004,* 2004,pp 392-402